



저작자표시-비영리-변경금지 2.0 대한민국

이용자는 아래의 조건을 따르는 경우에 한하여 자유롭게

- 이 저작물을 복제, 배포, 전송, 전시, 공연 및 방송할 수 있습니다.

다음과 같은 조건을 따라야 합니다:



저작자표시. 귀하는 원저작자를 표시하여야 합니다.



비영리. 귀하는 이 저작물을 영리 목적으로 이용할 수 없습니다.



변경금지. 귀하는 이 저작물을 개작, 변형 또는 가공할 수 없습니다.

- 귀하는, 이 저작물의 재이용이나 배포의 경우, 이 저작물에 적용된 이용허락조건을 명확하게 나타내어야 합니다.
- 저작권자로부터 별도의 허가를 받으면 이러한 조건들은 적용되지 않습니다.

저작권법에 따른 이용자의 권리는 위의 내용에 의하여 영향을 받지 않습니다.

이것은 [이용허락규약\(Legal Code\)](#)을 이해하기 쉽게 요약한 것입니다.

[Disclaimer](#)

Thesis for the Degree of Master of Engineering

**MONITORING OF ALGAL BLOOMS IN THE  
NAKDONG RIVER BY USING UNMANNED  
AERIAL VEHICLE(UAV) IMAGERY**



**Heung Min Kim**

**Department of Spatial Information Engineering**

**The Graduate School**

**Pukyong National University**

**February 2017**

**MONITORING OF ALGAL BLOOMS IN THE  
NAKDONG RIVER BY USING UNMANNED  
AERIAL VEHICLE(UAV) IMAGERY**

(무인항공기(UAV) 이미지를 이용한  
낙동강 녹조 모니터링)

**Advisor: Prof. Hong Joo Yoon**

**by**

**Heung Min Kim**

**A thesis submitted in partial fulfillment of the requirements  
for the degree of**

**Master of Engineering**

**in Department of Spatial Information Engineering,**

**The Graduate School,**

**Pukyong National University**

**February 2017**

**MONITORING OF ALGAL BLOOMS IN THE  
NAKDONG RIVER BY USING UNMANNED  
AERIAL VEHICLE(UAV) IMAGERY**

**A dissertation**

**by**

**Heung Min Kim**

**Approved by:**



**(Chairman) Prof. Kyung-Soo Han**



**(Member) Prof. Jin-Soo Kim**



**(Member) Prof. Hong-Joo Yoon**

**February 2017**

# CONTENTS

<b>CONTENTS</b> .....	i
<b>LIST OF FIGURES</b> .....	iii
<b>LIST OF TABLES</b> .....	iv
<b>ABSTRACT</b> .....	1
1. INTRODUCTION .....	3
2. DATA and Methods .....	8
2.1. Study Area .....	8
2.2. Methodology .....	10
2.2.1. UAV Imagery .....	12
2.2.1.1. UAV and Sensors Description .....	12
2.2.1.2. UAV Image Acquisition and Processing .....	15
2.2.2. Field measurement of Spectral Reflectance .....	22
2.2.3. Water Quality Exam .....	24
3. RESULTS .....	27
3.1. The Emergence Aspects of Phytoplankton .....	27
3.2. Image Detection Results Using Algal Bloom Index .....	32
3.3. The Emergence Aspects of Phytoplankton .....	44
4. CONCLUSION .....	47
5. REFERENCE .....	49

# LIST OF FIGURES

Figure 1. Location of the Nakdong River and survey area. ....	9
Figure 2. Flow chart in this study. ....	11
Figure 3. The UAV and Sensors used in this study. ....	13
Figure 4. Flight plan for aerial photography and photographing stations : (a) UAV imaging was started at position 1 and ended at position 12 and (b) Photographing stations of sensors. ....	17
Figure 5. (a) RGB and (b) NIR ortho image production through image preprocessing at 29 July 2015. ....	20
Figure 6. (a) RGB and (b) NIR ortho image production through image preprocessing at 18 August 2015 ....	21
Figure 7. Field spectral reflectance measurement using spectroradiometer : (a) Reference reflectance measurement using spectralon panel and (b) Water(fresh and algal bloom) reflectance measurement. ....	23
Figure 8. The distribution of sampling sites for water quality analysis in unmanned aerial photograph shooting range. ....	24
Figure 9. Field water sampling and obtaining coordinate information at each points. ....	26
Figure 10. The results of water quality exam : (a) The emergence aspects of phytoplankton and (b) Standing crop of phytoplankton at each sampling sites. ....	28

Figure 11. The shape of harmful cyanobacteria detected in the study area : (a) <i>Microcystis</i> sp. and (b) <i>Anabaena</i> sp. ....	30
Figure 12. The results of field spectral reflectance measurement using spectroradiometer : (a) Fresh water and (b) Algal Bloom. ·	34
Figure 13. Correlation analysis result between phytoplankton concentration and equation(3), (4) value. ....	38
Figure 14. Comparison of $\log(R_{850nm}/R_{660nm})$ (a) and $\log(R_{850nm}/R_{625nm})$ (b). .....	40
Figure 15. Detection results through the application of the calculated Algal bloom Index. ....	41
Figure 16. Correlation analysis result between phytoplankton concentration and algal bloom index value. ....	42
Figure 17. Sampling sites where water plants are distributed : (a) D-1, (b) D-2, (c) D-8 and (d) D-16. ....	43
Figure 18. Spatial distribution of algal bloom in the survey area photographed by UAV : (a) 29 July 2015 and (b) 18 August 2015. ....	46

## LIST OF TABLES

Table 1. Technical specifications of the UAV used in the present study(Sensefly, 2016) .....	12
Table 2. Technical specifications of the S110 RGB and NIR sensor (Sensefly, 2016) .....	14
Table 3. Results of ortho images generation .....	19
Table 4. The number of harmful cyanobacteria cells detected in each sampling sites(Unit : cells/mL) .....	31
Table 5. Criteria and indicators of algae bloom warning system .....	44
Table 6. Occurrence range of algal bloom at 29 July 2015 and 18 August 2015 .....	45

# 무인항공기 이미지를 이용한 낙동강 녹조 모니터링

김 흥 민

부경대학교 대학원 공간정보시스템공학과

## 요 약

부영양화 된 정체되어 있는 호소나 유속이 느린 하천에서 녹색이나 남색을 띠는 식물성 플랑크톤이 대량 번식하게 되면 녹조현상을 일으킬 수 있다. 녹조현상은 과거부터 현재까지 지속적으로 발생되고 있으며, 기후변화로 인한 수온 상승과 수환경이 오염되면서 그 발생 빈도 및 강도가 점점 증가하는 추세다. 녹조현상 발생에 따른 수질 오염은 최근 국내에서도 상수원 안전 문제에 대한 심각한 국민적 불안감 증폭으로 국가적 문제로 인식되고 있다. 이에 본 연구는 무인항공기를 이용한 녹조현상 모니터링 기법을 적용으로써 하천 수질환경 관리 능력을 향상시키는 데 목적이 있다.

한국의 4대강 중 하나인 낙동강 중류 권역을 대상으로 무인항공기를 이용한 원격탐사 자료를 취득하였다. 그리고 하천 저수 구역의 식물성 플랑크톤의 출현 양상을 파악하고 센서의 파장 대역 조합을 통한 녹조 탐지 지수식을 도출하기 위하여 수질 분석과 분광기를 이용한 현장 분광 반사도 측정을 수행하였다. 그 결과 Red(625 nm)와 NIR(850 nm)을 이용하는 것이 녹조 탐지에 효율적인 것으로 나타났으며, Red와 NIR 대역의 조합을 통해 얻은 녹조 탐지 결과 값과 조류 현존량간의 상관관계가 강한 양(+)의 상관관계를 가지는 것으로 나타났다. 그리고 전체 조사 수역에 대한 녹조현상의 공간적 분포를 분석한 결과 0.30 km<sup>2</sup> 면적에서 조류 경보 발령 기준의 경보(5,000 ~ 1,000,000 cells/mL 이상) 수준에 해당하는 강도를 보이는 것을 알 수 있었다.

본 연구를 통하여 수질 환경 모니터링에 무인항공기의 활용 가능성을 확인하였으며, 무인항공기를 이용한 원격탐사가 수질 오염 모니터링 기술이 실제 현장에 충분히 활용 가능할 것으로 사료된다. 향후 오염 정도에 따른 다양한 수면 상태에 대한 추가적인 수질 분석과 더불어 지속적인 분광 특성 연구를 통해 신뢰성을 높인다면 관리자들의 하천 수질 오염 초기 대응 능력을 향상시킬 수 있을 것으로 기대된다.



# 1. INTRODUCTION

Algae plays an important part in the aquatic ecosystem as the primary producer in the food chain. Algae uses sunlight for growth (photosynthesis), supplies oxygen to the aquatic ecosystem, and feeds on zooplankton (MOE, 2016). If industrial wastewater, livestock wastewater, domestic sewage, and so on are flowing into the water environment, photosynthesis in algae increases rapidly and can lead to eutrophication. During this phenomenon, algae mass proliferate in a short period, consuming excess oxygen in the water and creating an environment in which life cannot survive. Water bloom also occurs and further degrades water quality (Choe et al., 2011). Water bloom in lakes or rivers with slow flow velocity involves a change in water color to green due to the rapid increase in growth of algae such as Cyanobacteria, Chlorophyceae, and Bacillariophyceae (Park, 2015). Water bloom is called algal bloom or green tide (in Korea) in contradistinction to red tide in the sea.

Algae species that cause algal bloom include Cyanobacteria, Chlorophyceae, Euglenophyceae, Dinophyceae, and Bacillariophyceae (MOE, 2010). Cyanobacteria, which exhibit the most algal bloom (Park, 2014), proliferate at higher temperatures than other algae such as green algae, diatoms, etc. and have the ability to float on its own. In breeding environments, cyanobacteria float near the surface of the water and fall when they get enough nutrients. Using this

physiological advantage, cyanobacteria rapidly proliferate in and dominate eutrophic waters during the summer compared to other algae. When cyanobacteria float near the water surface, they produce toxins that kill other living organisms in the water and causes foul odors. This destroys aquatic ecosystems and results in various social, economic and environmental problems. For example, the occurrence of algal bloom in waters used as a water source can complicate water treatment and may alter the water taste and odor.

In addition to environmental factors, physical factors such as temperature, light, residence time, water flow, and mixing can cause algal bloom. Due to the climate in Korea, summer rainfall is concentrated and water outflow rates are high. Large dams and beams have been constructed to store water for use. If the flow rate is high, the flow is directed to another water storage area. If the flow rate is slowed and water residence time is lengthened, growth and accumulation of algae will increase and likely lead to algal bloom (Park, 2014).

Algal bloom has continuously been occurring from the past to the present, but with the rise of water temperature and pollution in the water environment, the frequency and severity is increasing even more (Senhorst and Zwolsman, 2005; Gregory, 2006; Bates *et al.*, 2008; Thackeray *et al.*, 2008; Park, 2014). In Korea, water pollution caused by algal bloom has currently been bringing serious anxiety of people over safety of water supply sources and it is now being

recognized as a national issue (Kim *et al.*, 1989; Kim *et al.*, 1998; Paerl and Huisman, 2008;). In the Korean peninsula, four main rivers of Han River, Geum River, Nakdong River and Youngsan River are flowing across the country, and particularly in the case of Han River and Nakdong River, major big cities have been developed along the rivers which have been major sources of water supply for agricultural, industrial and drinking uses (Park, 2012). However, with worsening of eutrophication, continuous heat and drought, algal bloom in the water has increased, and it raised continuous water quality issues (Srivastava *et al.*, 2015). The occurrence of green algae in rivers and streams used as water sources can have a great impact on water treatment, such as clogging of filter papers and formation of total trihalomethane (THM), a carcinogenic substance, due to excess chlorine treatment. In addition, algae cause discomfort and public hygiene problems, and can disrupt various water leisure activities. Disruption of leisure activities, lack of water, etc. can result in great losses to the local economy. Therefore, to address the overuse of drinking water and maintaining a stable supply of water by securing clean water sources, the need to develop technologies to prevent water pollution caused by algal bloom is urgent. Furthermore, capabilities to deal with the emergence and distribution of algal bloom preemptively through regular forecasting and effective monitoring activities must be enhanced.

Currently, monitoring of algal bloom in Korea is conducted through

local sampling in field investigations and aerial forecasting using manned vehicles. Sampling investigations are effective in identifying the severity and conditions of algal bloom. However it costs a lot of time and research personnel, and it is not possible to identify spatial distribution such as the volume of emergence and expansion due to the characteristics of local investments (Su and Chou, 2015). In the case of aerial forecasting using manned vehicles and satellites, the existing remote sensing method is effective for observing a wide space in a short period. But, the limitation is that it costs a very high price for the operation and that it is difficult to use regularly (Hakala *et al.*, 2010). When massive algal bloom occurs, aerial forecasting can provide information about the spatial expansion in the wide range, but when it comes to small and medium range of algal bloom around a river, interpretation can be difficult. Therefore, in order to enhance the capability to deal with emergence of algal bloom preemptively, it is required to develop a new kind of forecasting and monitoring system which can overcome limitations of the existing methods.

To supplement the existing remote sensing method, various data are acquired using an unmanned aerial vehicle (UAV). Recently, the remote sensing technique using UAV has been applied in many fields as an innovative multi-purpose tool for acquiring various data including geospatial information (Su *et al.*, 2015; Jang *et al.*, 2015; Tianyun *et al.*, 2015). A UAV, also called a drone, is a motorized

aircraft that does not require a pilot and can be controlled via radio signals. The UAV roadmap, published by the US Defense Secretary, defines the aircraft as a "one-time or recyclable power vehicle that does not burn a pilot, but is powered by aerodynamic forces, flying autonomously or remotely" (OSD, 2003).

Recently, the remote sensing method using UAV is applied in various areas as an innovative multi-purpose tool to obtain data including geo-spatial information (Su *et al.*, 2015; Jang *et al.*, 2015; Tianyun *et al.*, 2015). Remote sensing method using UAV can implement operations regularly whenever necessary at a lower cost compared to manned vehicles or satellites to obtain spatio-temporal data in high resolution (Laliberte *et al.*, 2007; Dunford *et al.*, 2009; Berni *et al.*, 2009; Del Pozo *et al.*, 2014). Besides, with its excellent mobility, it can be applied in places with difficult accessibility for human or in dangerous environments (Jang and Roh, 2005, Everaerts, 2008; Jang *et al.*, 2011). In this aspect, this UAV can be a new solution to supplement disadvantages of conventional remote sensing and field investigation methods.

This study attempts to develop algal bloom monitoring technology using UAV which can implement effective interpretation of spatial distribution at a relatively lower cost compared to aerial forecasting and can overcome visual and spatial limitations of sampling investigation in order to improve controlling capability of river water quality and environment.

## 2. DATA and METHODS

### 2.1 Study Area

Nakdong River locates at the southern east part of the Korean Peninsula and is the second largest river in Korea with length of 521.5 km and size of 23,717 km<sup>2</sup> (Jang *et al.*, 2014; Figure 1a). Total quantity of Nakdong River is 385 tons per year, and 9.5 billion tons (24.7%) of water for use (industrial, agricultural, living and drinking purposes) are supplied to big cities converged with major industries and population such as Busan and Daegu Metropolitan Cities (MOE, 2016). In the midstream and downstream where these big cities locate, water pollution is frequently occurring due to increased inflow of sewage and aggravation of eutrophication (Srivastava *et al.*, 2015). The present study targeted the midstream area of Nakdong River, in which all the administrative districts of Daegu Metropolitan City are located with high dependency of water resource uses and with frequent occurrence of algae related water pollution (Figure 1b). Among the midstream areas of Nakdong River, the selected site for the study is Dodong-ri, Guji-Myeon, Dalseong-gun, Daegu (Figure 1c), which was covered by Korean media several times due to the frequent occurrence and severity of algal bloom (e.g. SBS TV, 2012, SBS TV, 2013; Yonhap News, 2014; Yonhap News, 2015).

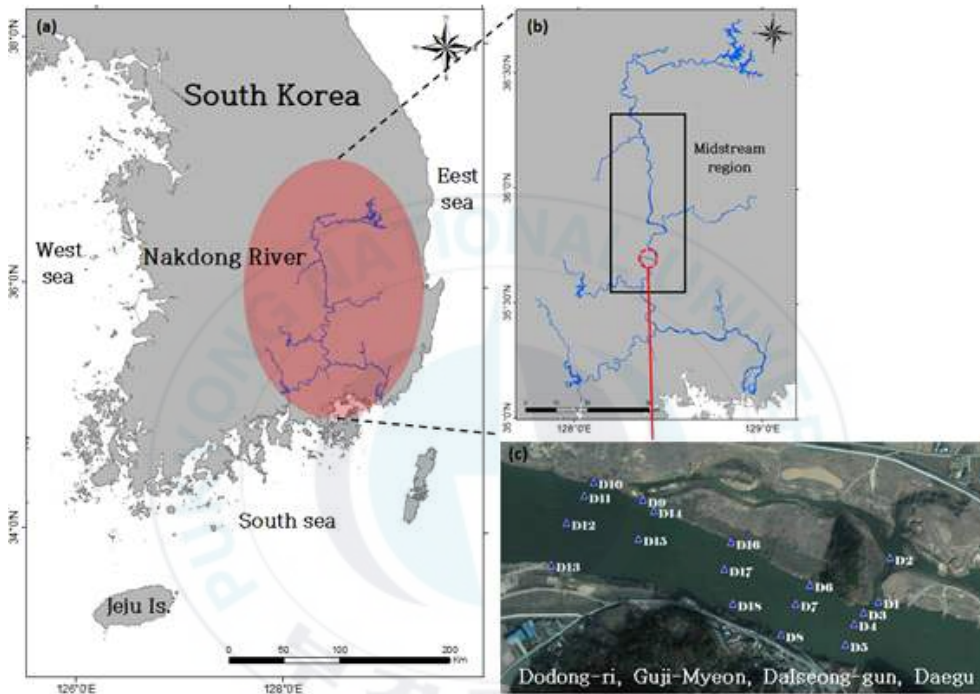


Figure 1. Location of the Nakdong River and survey area.

## 2.2 Methodology

Figure 2 shows the flowchart of this study. A spectrum survey of algal bloom and clear water, image acquisition using UAV, and a water quality exam and sampling were conducted in the study area. After obtaining spectroscopic characteristics of the algal bloom and the fresh water, the algal bloom detection index was calculated. Images were acquired using unmanned aerial photography, and were processed as a single orthoimage that was produced using an image preprocessing technique. The index value was then calculated using band combination of the orthoimage. The correlation between the calculated index value and the abundance of phytoplankton concentration during the water quality test was analyzed. Finally, algal bloom was detected using the index equation with a high correlation coefficient.

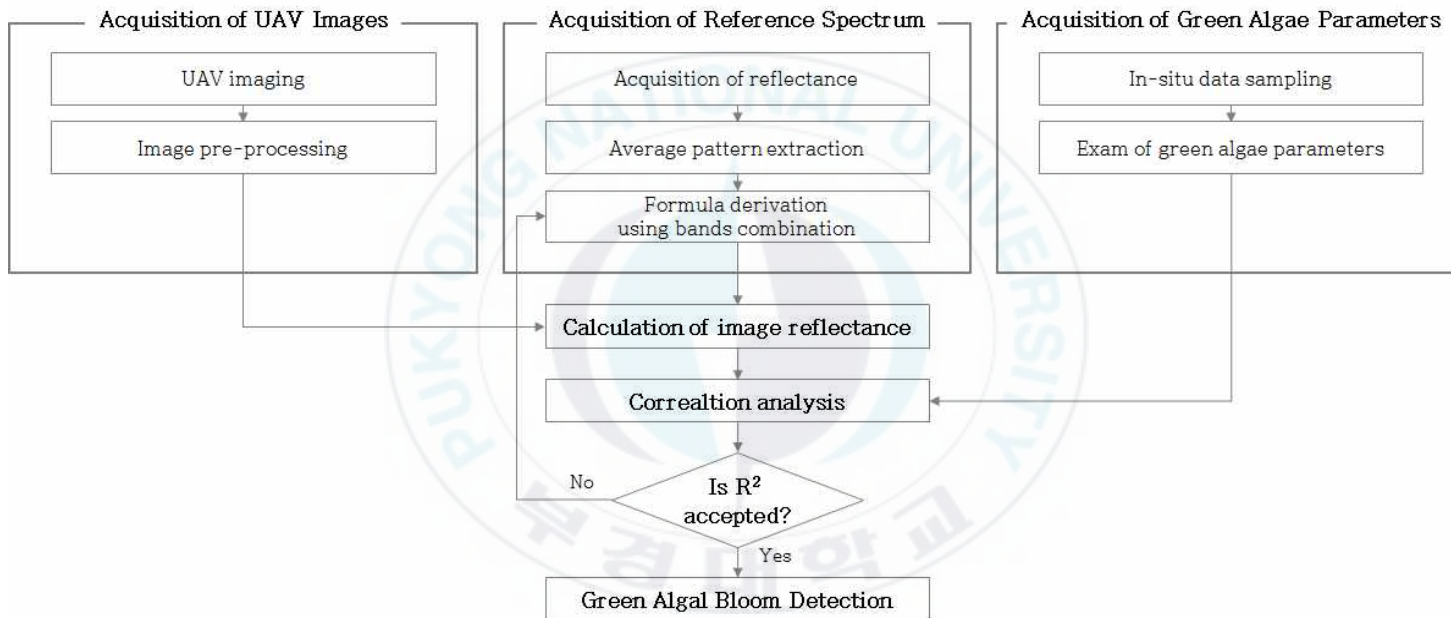


Figure 2. Flow chart in this study.

## 2.2.1 UAV Imagery

### 2.2.1.1 UAV and Sensors Description

The unmanned aerial vehicle (UAV) used in this study is Sensefly Ltd's eBee (Figure 3a) which can make a long flight (single flight: 12 km<sup>2</sup> at 974 m altitude) and can obtain high resolution images (Ground Sampling Distance : down to 1.5 cm per pixel) (Sensefly, 2016).

eBee is a fixed wing UAV, with function of automatic flight using flight control software, GPS of the vehicle and IMU as well as the function of manual operation. The specification of eBee can be found in Table 1.

Table 1. Technical specifications of the UAV used in the present study (Sensefly, 2016)

<b>Weight</b>	Approx. 0.69 kg
<b>Wingspan</b>	96 cm
<b>Maximum flight time</b>	50 min
<b>Radio link range</b>	Up to 3 km
<b>Flight altitude</b>	100 ~ 800 m
<b>Maximum coverage(single flight)</b>	12 km <sup>2</sup>
<b>Wind resistance</b>	12 m/s
<b>Nominal cruise speed</b>	40-90 km/h
<b>Ground Sampling Distance</b>	Down to 1.5 cm per pixel



Figure 3. The UAV and Sensors used in this study.

Next, for the sensors to install in UAV for obtaining image materials, Canon Powershot S110 RGB and NIR were selected (Figure 3b). The specification of S110 RGB and NIR sensor can be found in Table 2. S110 RGB sensor basically has the function of digital camera and provides standard band data of Red (660 nm), Green (520 nm) and Blue (450 nm) to enable visible spectrum analysis of images. S110 NIR sensor consists of NIR (850 nm) band used to calculate NDVI (normalized difference vegetation index) for assessing biomass and plant health, apart from Green (550 nm) and Red (625 nm) band.

Table 2. Technical specifications of the S110 RGB and NIR sensor (Sensefly, 2016)

	S110 RGB	S110 NIR
<b>Size</b>	7.44 × 5.88 mm	
<b>Weight</b>	0.7 kg	
<b>Resolution</b>	12 million pixels	
<b>Image Format</b>	JPEG / RAW	
<b>Band</b>	Red(660nm), Green(520nm), Blue (450 nm)	Red(625nm), Green(550nm), NIR(850nm)

### 2.2.1.2 UAV Image Acquisition and Processing

Adequate flight planning for UAV is a very important part to acquire high quality data to meet the purpose of using the vehicle (Del Pozo *et al.*, 2014). In aerial photography, the degree of redundancy of photographs was set to 60% in the direction of the shooting progress (longitudinal overlap) and 30% in the adjacent courses (lateral overlap). A longitudinal overlap of 60% for stereoscopic photography and pass points is the minimum overlap required for aerial triangulation. However, the overlap can be modified as needed.

In this study to monitor algal bloom in the river, mission parameters for the photographic flight of UAV were established as follows: flight height - 400 m (ground resolution: 14 cm/pixel), single flight time - within 20 minutes, Flight strip - rectangular route (11 line) (Figure 5a). To generate orthomosaic images of the photographed area, the camera was set as follows: pixel size - 1.86  $\mu\text{m}$ , focal length - 4.4 mm, lateral overlap - 75%, longitudinal - 70%.

The actual monitoring of Nakdong River water area of Dodong-ri, Guji-Myeon, Dalseong-gun, Daegu (Figure 1c) was conducted two times on July 29<sup>th</sup> and August 18<sup>th</sup> 2015 when high severity of algal bloom continued since the first observation on June 10<sup>th</sup> 2015 by the media (eg. E-today News, 2015; MBC TV, 2015; Yonhap News, 2015).

As eBee is made of EPP foam material and has a light weight of

0.69 kg, it is not possible to mount 2 sensors at the same time for a long flight. For this reason, the researcher mounted S110 RGB and NIR separately for each time of monitoring to acquire image data. In order to conduct monitoring of the river's reservoir area including the surrounding areas in a single flight, 57 photographing stations were required, and individual images with 4,000(width) × 3,000(height) pixels were acquired (Figure 4b).



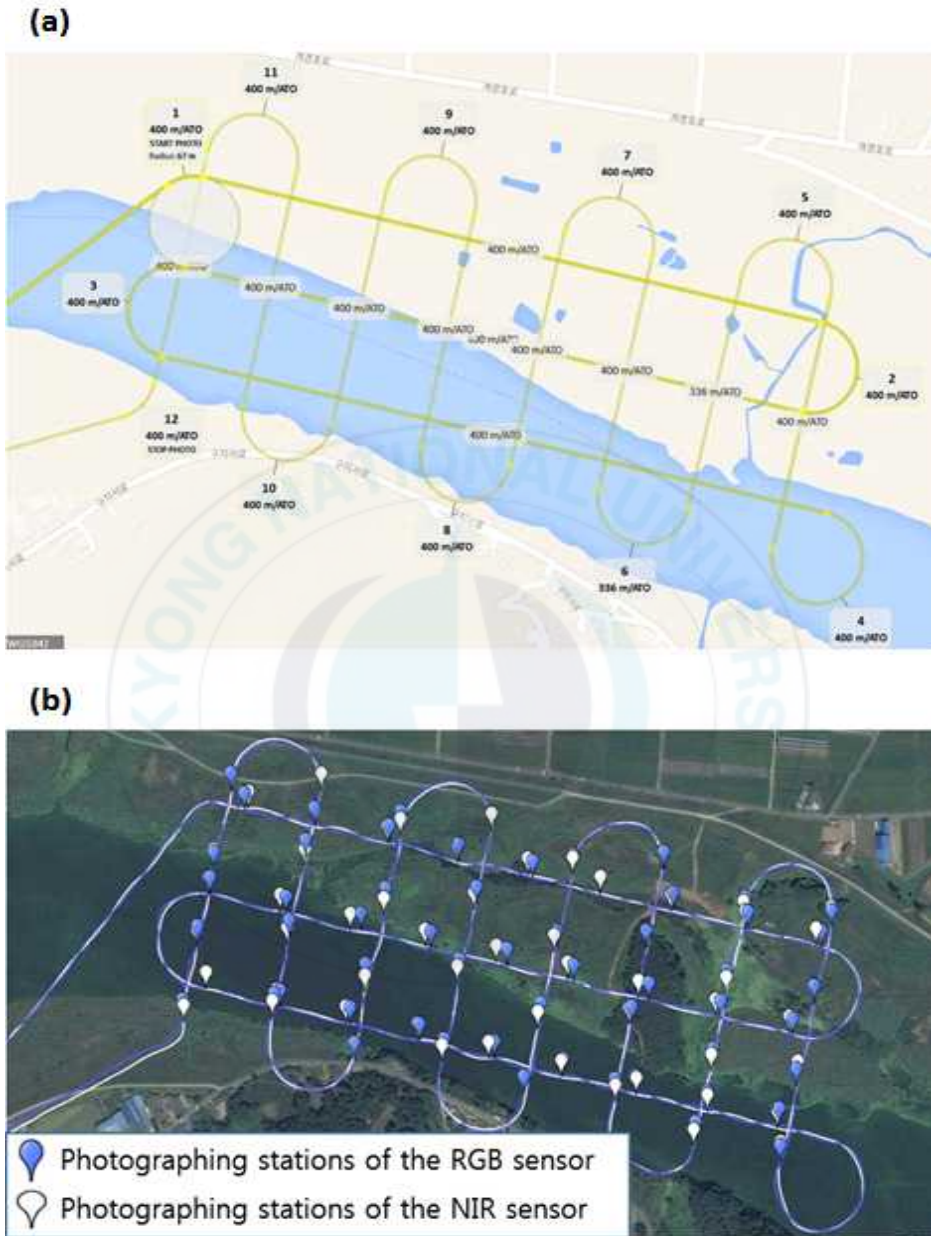


Figure 4. Flight plan for aerial photography and photographing stations : (a) UAV imaging was started at position 1 and ended at position 12 and (b) Photographing stations of sensors.

Geotagging, georeferencing, and orthomosaic generation are required for the analysis of images acquired by aerial photography. Geotagging refers to the process of using GPS to add geographic information to images during photography. Georeferencing, or geometric correction, is an image processing technique that corrects the geometric distortion of the image by the sensor attitude, the error of the observation device, the terrain flexure, etc., and converts the distortion into a specific coordinate system when acquiring the image using remote sensing. Using the geometrically corrected image, the image is matched to a single image and projected on a complete plane to produce an orthoimage that can accurately calculate the area of the image by the same scale.

Individual images acquired through S110 RGB and NIR were implemented processes of geotagging and georeferencing through flight logs (latitude, longitude, altitude, accuracy horz (m), accuracy vert (m), etc.), which were recorded automatically by GPS and IMU sensors. Besides, in order to identify spatial distribution of algal bloom within the photographed reservoir area of the river, the researcher produced an orthomosaic image by matching georeferenced images (Figure 5, 6). The information of orthomosaic images photographed on July 29<sup>th</sup> and August 18<sup>th</sup> 2015 are shown in Table 3.

Table 3. Results of ortho images generation

	2015.07.29.	2015.08.18
<b>Average Ground Sampling Distance(GSD)</b>	12.98 cm	12.9 cm
<b>Area Covered</b>	0.6291 km <sup>2</sup>	0.5847 km <sup>2</sup>
<b>Image Coordinate System</b>	WGS84	WGS84
<b>Output Coordinate System</b>	WGS84/UTM 52N	WGS84/UTM 52N

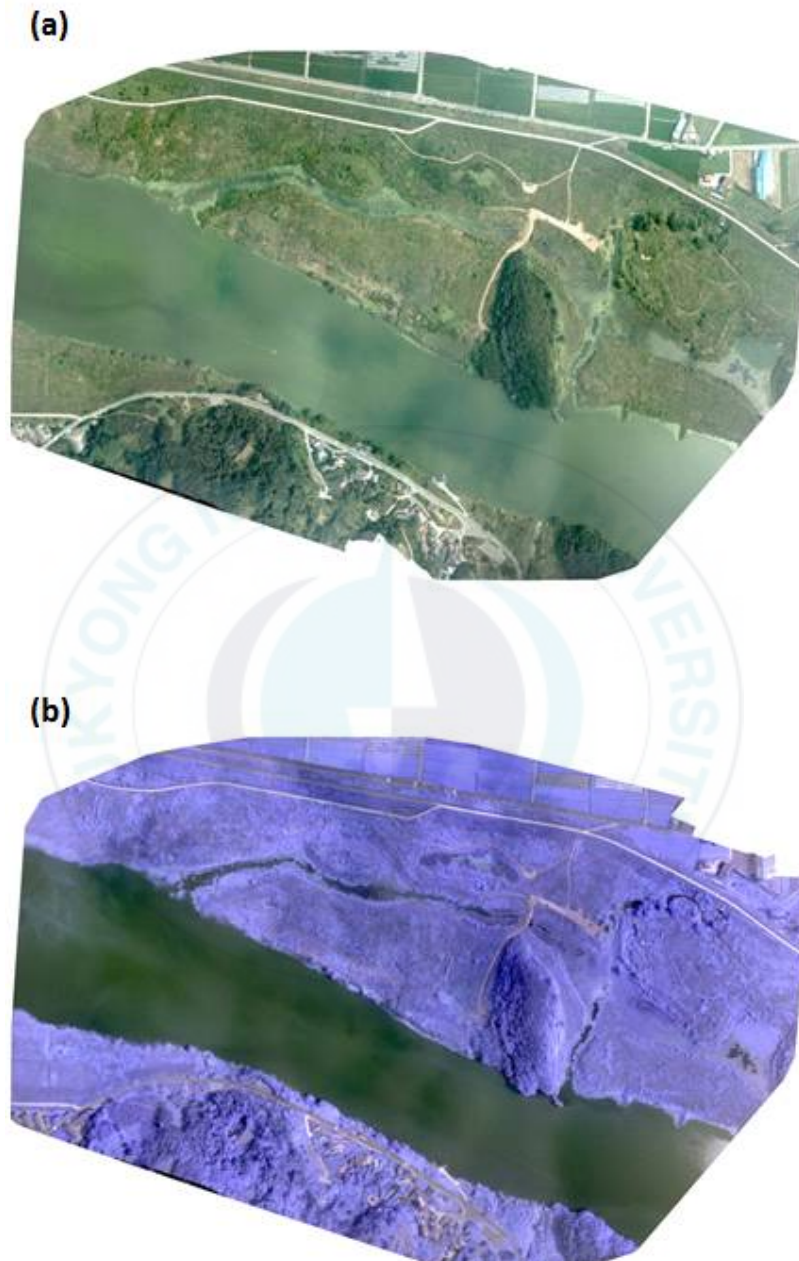


Figure 5. RGB(a) and NIR(b) ortho image production through image preprocessing at 29 July 2015.

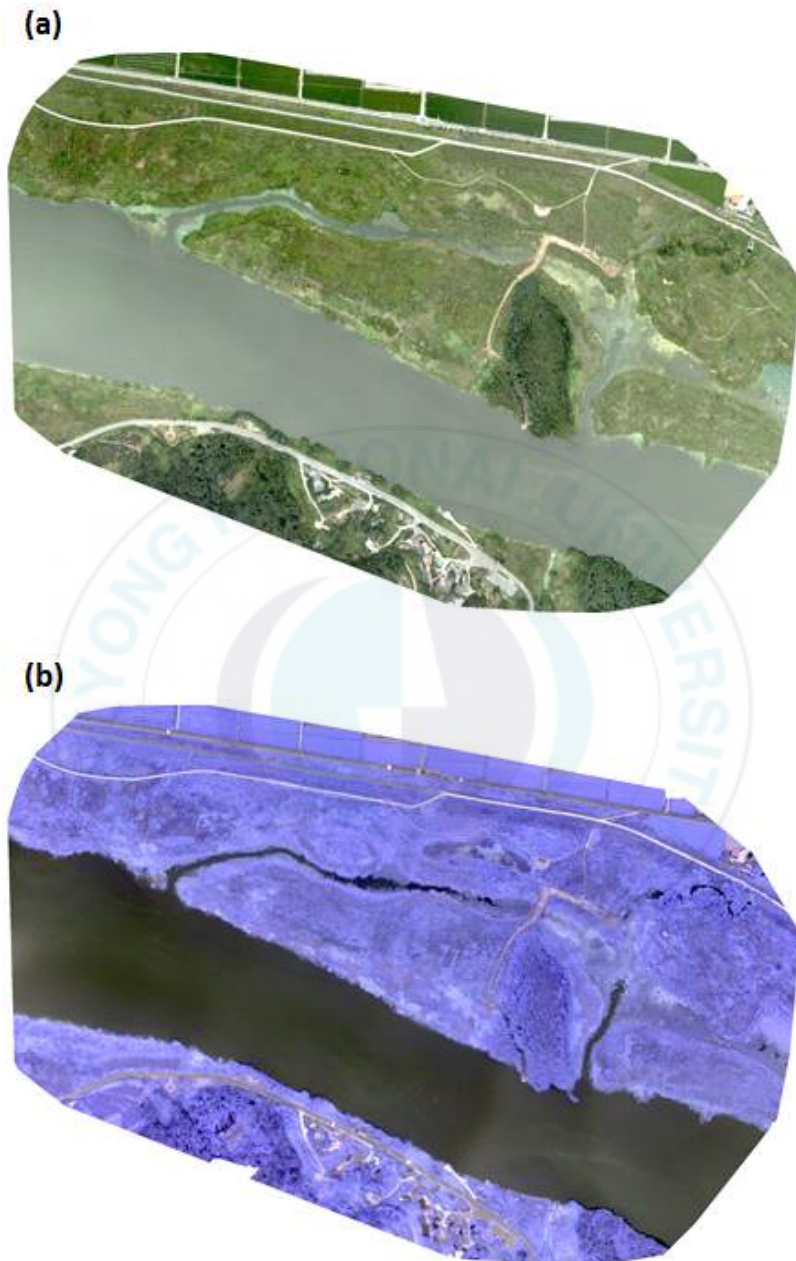


Figure 6. RGB(a) and NIR(b) ortho image production through image preprocessing at 18 August 2015.

## 2.2.2 Field Measurement of Spectral Reflectance

The researcher conducted field spectral reflectance on reservoir area of the river using spectroradiometer to investigate algal bloom within the images generated from wavelength band mixing of UAV sensors. For measuring field spectral reflectance, the spectroradiometer was used with functions of wavelength range of 325 nm - 1075 nm, an accuracy of  $\pm 1$  nm and a resolution of  $< 3$  nm at 700 nm (FieldSpec<sup>®</sup> HandHeld2, ASD inc., USA). The researcher measured basic reflectivity using Spectralon panel (10×10-inch) with 99% reflectivity, and each reflectivity of totally 30 sites including 18 sites of water collection were measured (Figure 7). In order to minimize any noise from wind and so on at the point of measurement, the researcher measured 5 times at each site and used the mean value of the measured values.



Figure 7. Field spectral reflectance measurement using spectroradiometer : (a) Reference reflectance measurement using spectralon panel and (b) Water(fresh and algal bloom) reflectance measurement.

### 2.2.3 Water Quality Exam

To identify emergence aspects of phytoplankton in the reservoir area of the river photographed by UAV and to examine the results of image detection by integrating the sensor's wavelength band mixing, the researcher conducted field investigation and quantity analysis of 18 sites on July 29<sup>th</sup> 2015 (Figure 8).

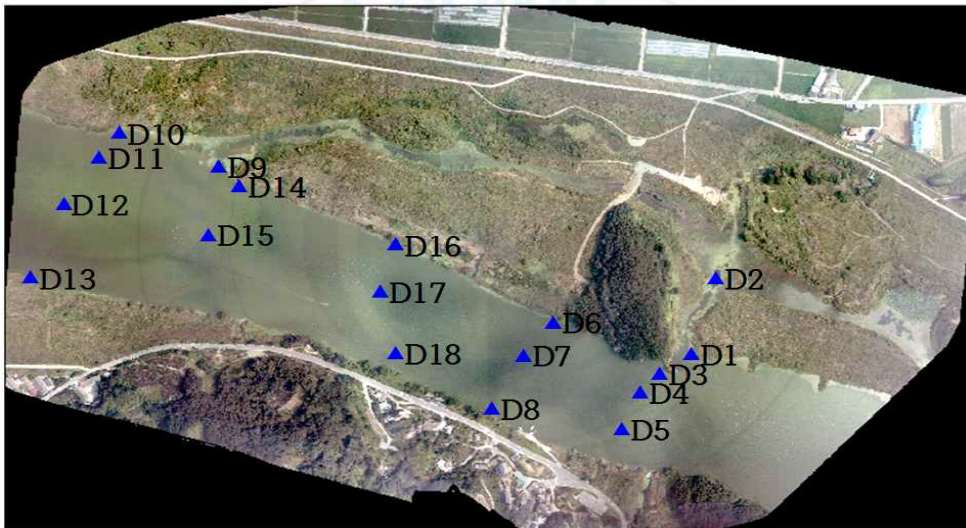


Figure 8. The distribution of sampling sites for water quality analysis in unmanned aerial photograph shooting range.

For collection of water, the researcher made judgments about visually polluted sites and relatively unpolluted sites and filled in 1,000 mL bottles at each site while moving the sites by boat. At the same time, by using GPS, the researcher acquired location information of each site. The samples of collected water bottles were fixed with Lugol's solution at the site, and in order to prevent photo-oxidation, aluminum foils were wrapped around the bottle to shut off from the lights (Figure 9). Then, after precipitating the water in centrifuge tube for 48 hours, the researcher removed the supernatant and concentrated the water to 10 mL liquid. Sedgwick-Rafter Counting Chamber was used to yield the coefficient and it was indicated in the converted figures of emergence per unit volume (cells/mL). For species identification, the researcher used high magnification optical microscope (Motic BA210) to conduct analysis up to species level. In the case when the identification up to species level was difficult, the identification was conducted up to the upper level classification.



Figure 9. Field water sampling and obtaining coordinate information at each points.

## 3. RESULTS

### 3.1 The Emergence Aspects of Phytoplankton

The species composition of phytoplankton emerged in the investigated water showed to be 16 species of 5 classification group. Among them, *Cyanophyceae* and *Chlorophyceae* accounted for the biggest proportion with 5 species (31.3%) each, and followed by *Bacillariophyceae*, *Euglenophyceae*, and *Dinophyceae*, each of which with 1 species (Figure 10a). The result of analyzing the quantity of phytoplankton showed that the total standing crop was 9,639,001 cells/mL. Among this, *Cyanophyceae* accounted for 99.9% (9,637,026 cells/mL) and the standing crops of other species were very low. When the standing crops of each collected site were compared, Site 10 showed the highest standing crop with 23,230 ~ 2,273,800 cells/mL (mean value - 535,500 cells/mL) and Site 15 showed the lowest one (Figure 10b).

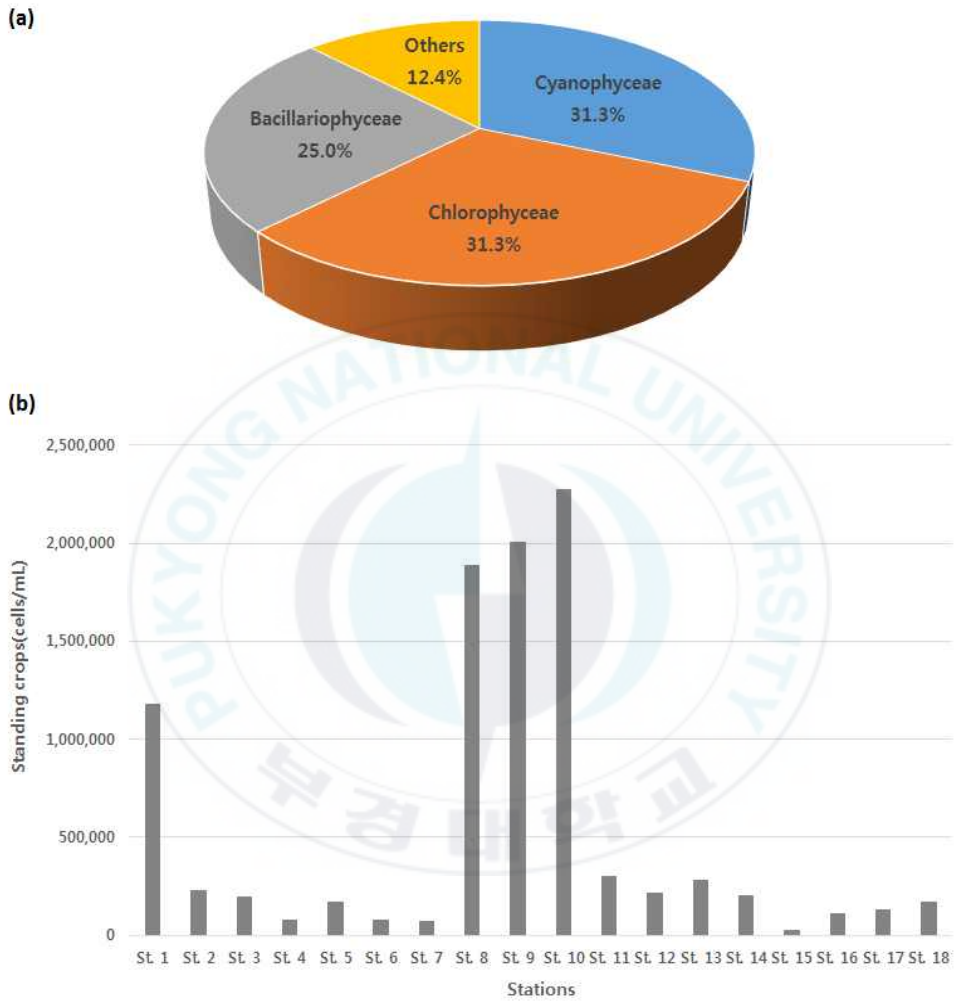


Figure 10. The results of water quality exam : (a) The emergence aspects of phytoplankton and (b) Standing crop of phytoplankton at each sampling sites.

*Cyanophyceae*, which showed the highest standing crop, contains blue-green protein and cause algal bloom making the color of water dark green. Some of *Cyanophyceae* emit smelling material and small amount of toxin, which cause harm to the health. Ministry of Environment has designated and is managing 4 species of *Cyanophyceae* including *Microcystis* sp., *Anabaena* sp., *Oscillatoria* sp., and *Aphanizomenon* as harmful cyanobacteria (MOE, 2015). In the investigated area, among the 4 species of harmful cyanobacteria, *Microcystis* sp. (Figure 11a) and *Anabaena* sp. (Figure 11b) appeared as dominant species with 8,502,525 cells/mL (88.2%) and 1,076,967 cells/mL (11.2%) respectively. The cell quantities of harmful cyanobacteria at each collected site are shown in Table 4.

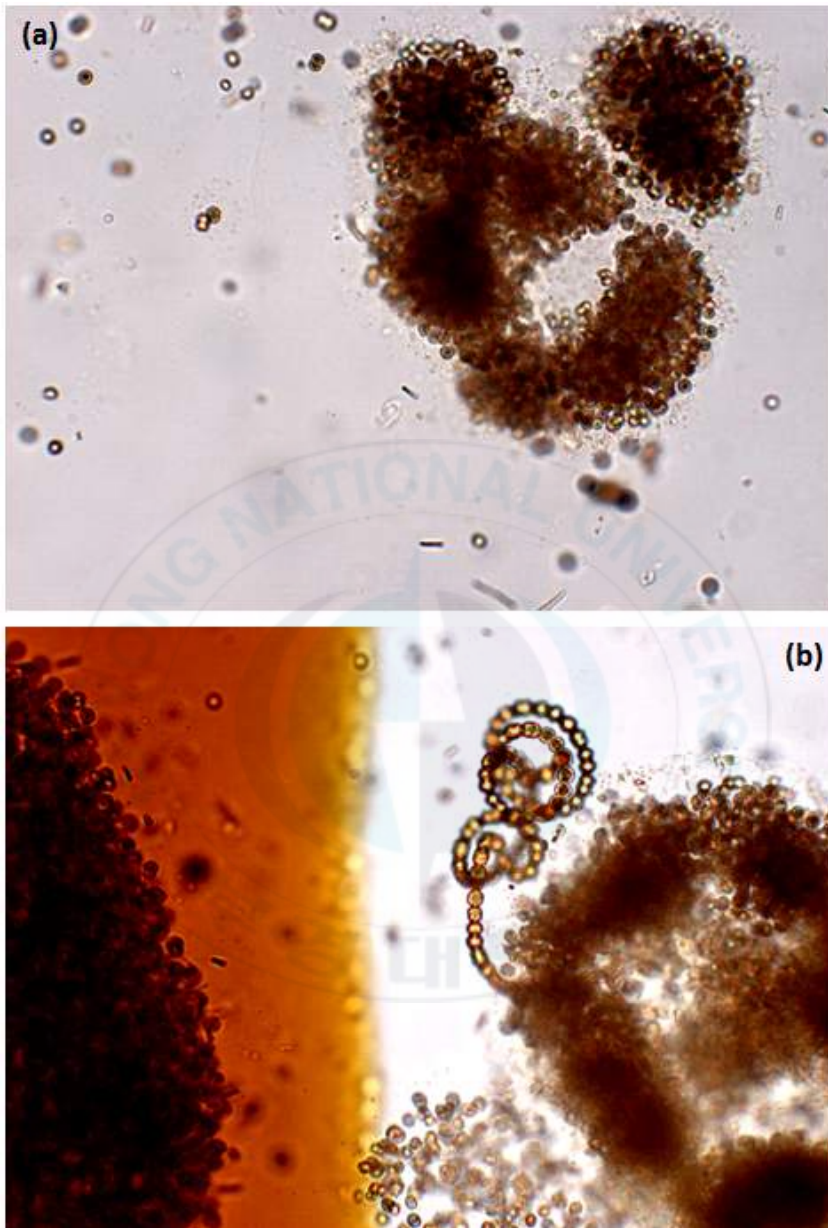


Figure 11. The shape of harmful cyanobacteria detected in the study area : (a) *Microcystis* sp. and (b) *Anabaena* sp.

Table 4. The number of harmful cyanobacteria cells detected in each sampling sites(Unit : cells/mL)

		Harmful cyanobacteria			Total
		<i>Microcystis</i> sp.	<i>Anabaena</i> <i>crassa</i>	<i>Anabaena</i> sp.	
Sampling sites	St. 1	1,178,361	0	0	1,178,361
	St. 2	227,174	33	0	227,207
	St. 3	197,376	0	0	197,376
	St. 4	73,728	577	4,363	78,668
	St. 5	160,358	0	7,920	168,278
	St. 6	70,464	0	7,080	77,544
	St. 7	66,864	0	0	66,864
	St. 8	1,879,680	0	8,400	1,888,080
	St. 9	1,605,120	0	401,280	2,006,400
	St. 10	1,818,960	0	454,740	2,273,700
	St. 11	222,720	0	74,239	296,959
	St. 12	212,486	0	0	212,486
	St. 13	222,984	0	55,746	278,730
	St. 14	159,408	0	39852	199,260
	St. 15	20,582	0	2,572	23,154
	St. 16	94,147	0	15,691	109,838
	St. 17	126,547	0	1,204	127,751
	St. 18	165,564	0	3,878	169,442
<b>Total</b>		8,502,523	610	1,076,965	9,580,098

## 3.2 Image Detection Results Using Algal Bloom Index

The reflectivity of natural light reflected from the water surface changes depending on the condition of the surface. The investigated water areas can be broadly divided into conditions of relatively clear water and algal bloom emerged water, and there were differences in the reflectance depending on the condition of water surface in each site. As the quantity and quality of materials contained in the water surface can be different, the color or reflection of the water surface, i.e the signal strength of dispersed light is not same. Therefore, when it is measured by spectroradiometer, the resulting value can be different each time (Kim, 2007).

For remote sensing applications, researchers have extensively used the accessory photopigment, phycocyanin, as the marker pigment for estimating the presence of cyanobacteria (Dekker, 1993; Simis *et al.*, 2005, Mishra *et al.*, 2009, 2013). Phycocyanin is a pigment that is present primarily in cyanobacteria and can be used as an indicator of cyanobacteria (Kutser *et al.*, 2006). Chlorophyll-*a* is present as a major pigment present in cyanobacteria as well as phycocyanin, and both of these pigments exhibit strong absorption in the red band. In addition, high reflectance peak in the near infrared bands is mostly affected by the multi-scattering effects related to the cell structure of cyanobacteria (Han *et al.*, 2010). Using these spectroscopic properties,

a specific substance present on the surface of the water can be detected.

Figure 12 shows the graph of reflectance data measured in the conditions of relatively clear water surface and algal bloom emerged water surface.



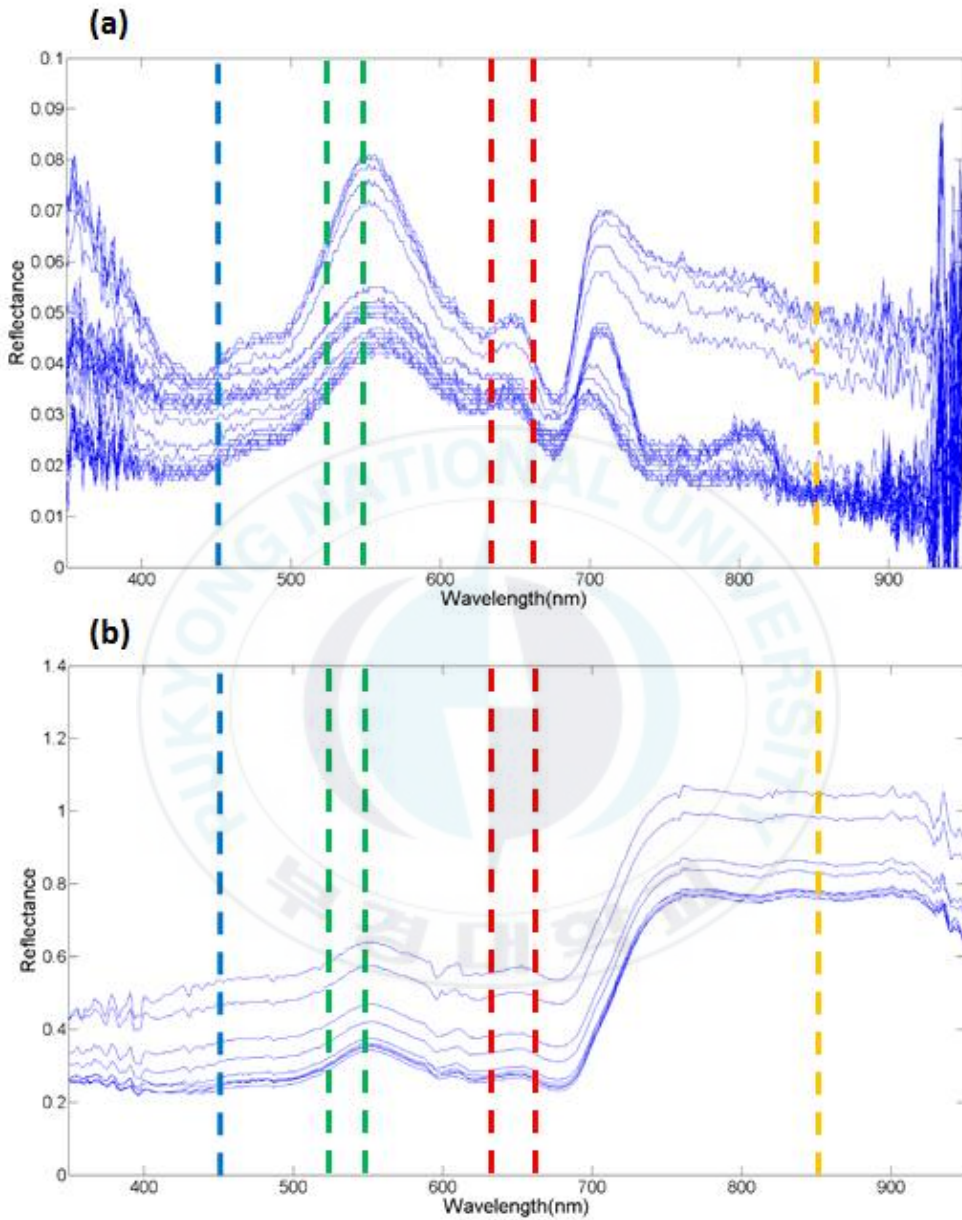


Figure 12. The results of field spectral reflectance measurement using spectroradiometer : (a) Fresh water and (b) Algal bloom.

When we examine the features of reflectance, the water surface in clear condition shows reflectance of 0.02 to maximum 0.08 in the range from Blue band to NIR band, and the reflectance by channels does not show significant difference (Figure 12a). However, in the case of algal bloom water, within the visible light, it showed the low reflectance of 0.23 in Red band and showed the reflectance not lower than 0.7 in NIR band (Figure 12b). These results show that a local minima near 630 nm caused by phycocyanin absorption, a small peak near 650 nm and high reflectance values around 700 nm are the typical features in the reflectance spectra of waters dominated by cyanobacteria (Reinart *et al.*, 2006). It is effective to use a Red band having a low reflectance value and an NIR band having a high reflectance value when detecting algal bloom. Therefore, using the Red and NIR bands, the following equation can be calculated :

$$AI_1 = (R_{\lambda_1} - R_{\lambda_2}) / (R_{\lambda_1} + R_{\lambda_2}) \quad (1)$$

$$AI_2 = \log(R_{\lambda_1} / R_{\lambda_2}) \quad (2)$$

where :

$AI$  Algal bloom Index

$R_{\lambda_1}$  represents the reflectance at NIR

$R_{\lambda_2}$  represents the reflectance at red

Considering the available bands in this study, the following can be calculated using the Red band at 625 nm, a band at 660 nm, and the NIR band at 850 nm :

$$AI_1 : \tag{3}$$

$$(R_{850\text{nm}} - R_{660\text{nm}}) / (R_{850\text{nm}} + R_{660\text{nm}})$$

$$(R_{850\text{nm}} - R_{625\text{nm}}) / (R_{850\text{nm}} + R_{625\text{nm}})$$

$$AI_2 : \tag{4}$$

$$\log(R_{850\text{nm}} / R_{660\text{nm}})$$

$$\log(R_{850\text{nm}} / R_{625\text{nm}})$$

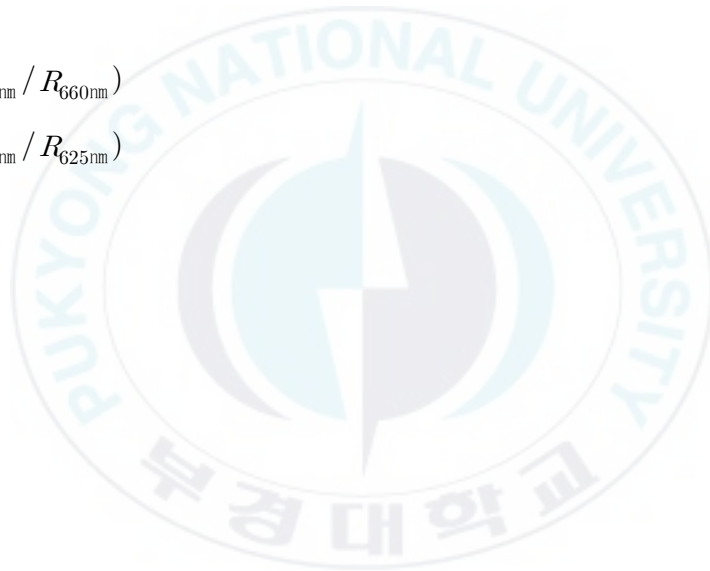


Figure 13 is a graph analyzing the correlation analysis result between phytoplankton concentration and equation (3), (4) value. In the  $AI_1$  equation, the correlation coefficient (R) between the phytoplankton concentration and the index value at 850 nm and at 660 nm was 0.4664, and (R) between the phytoplankton concentration and the index value at 850 nm and at 625 nm was 0.58. In the  $AI_2$  equation, (R) between the phytoplankton concentration and the index value at 850 nm and at 660 nm was 0.5188, and (R) between the phytoplankton concentration and the index value at 850 nm and 625 nm was 0.7874.

In the  $AI_1$  and  $AI_2$  equations, the index values using the 625 nm wavelength compared to those using the 660 nm wavelength was highly correlated with the phytoplankton concentration. Based on these results, the 625 nm wavelength is more efficient than the 660 nm wavelength for detecting algal bloom. In addition, the index value calculated with  $AI_2$  rather than that calculated with  $AI_1$  showed a relatively high (R). Therefore  $AI_2$  is effective in detecting algal bloom.

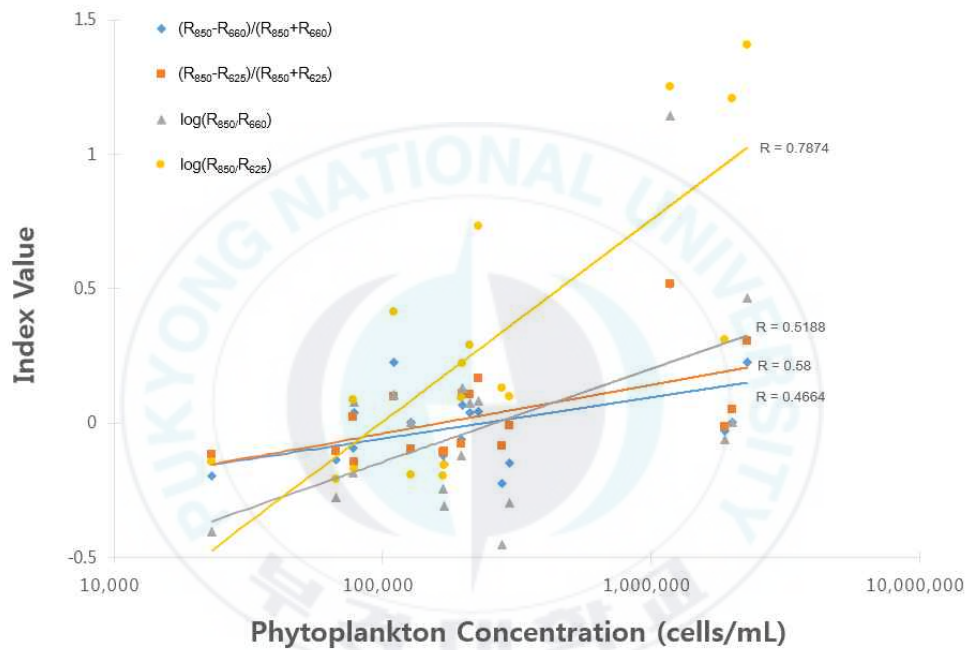
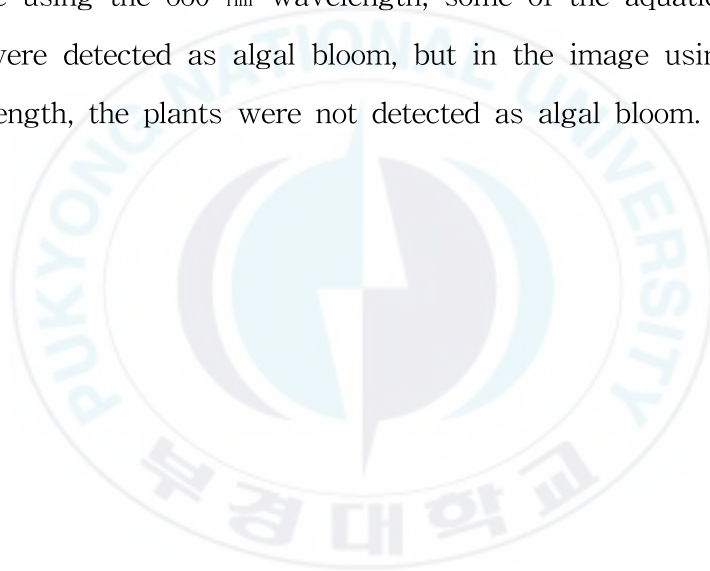


Figure 13. Correlation analysis result between phytoplankton concentration and equation(3), (4) value.

$AI_2$ , which has higher correlation coefficient than  $AI_1$ , was used to detect the algal bloom (Figure 14). The images using the 660 nm wavelength showed that the algal bloom was concentrated on the left side of the image corresponding to the downstream of the river (Figure 14a). However, in the image using the 625 nm wavelength, algal bloom was concentrated in the center and on the right side of the image corresponding to the upstream of the river (Figure 14b). In the image using the 660 nm wavelength, some of the aquatic plants in area A were detected as algal bloom, but in the image using the 625 nm wavelength, the plants were not detected as algal bloom.



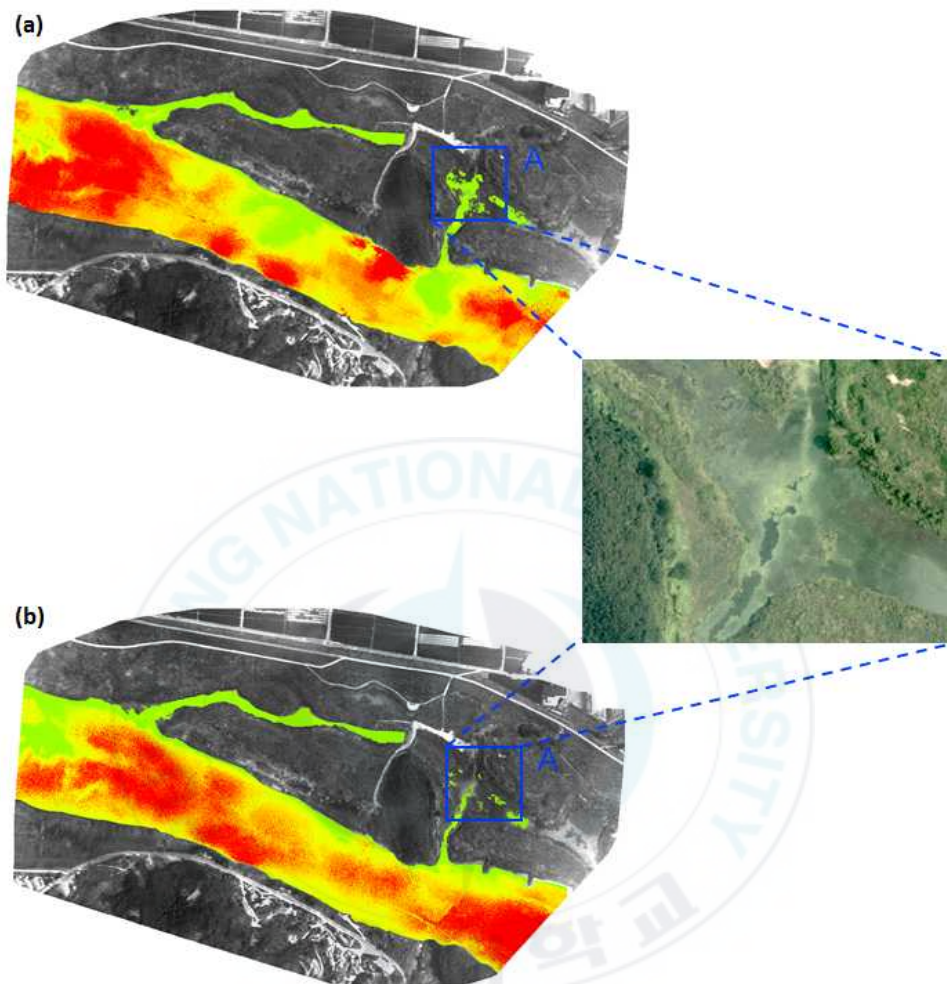


Figure 14. Comparison of  $\log(R_{850\text{nm}}/R_{660\text{nm}})$  (a) and  $\log(R_{850\text{nm}}/R_{625\text{nm}})$  (b).

From the above results, the Algal bloom Index derived from this study can be calculated as equation (5) :

$$AI = \log(R_{850\text{nm}}/R_{625\text{nm}}) \quad (5)$$

The results obtained by applying the induced Algal bloom Index (5) are shown in Figure 15. The applied date was July 29<sup>th</sup> 2015 when unmanned aerial photographing, water collecting in the field and measuring of spectral reflectance were conducted at the same time.

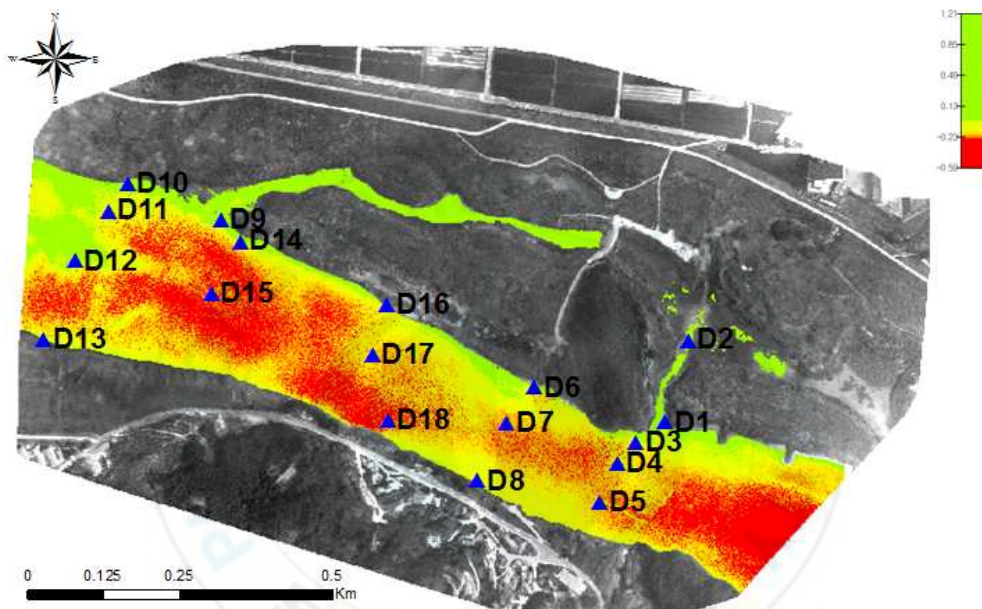


Figure 15. Detection results through the application of the calculated Algal bloom Index.

Except for the water surface, the land areas are inactivated, and the values of detected results are indicated in the form of index from -0.59 to 1.21 with no unit. The result of comparing Algal bloom Index and standing crops at each water collected site mentioned in 3.1 showed that the quantity of algae was smallest in D-15 with

23,230 cells/mL. The index value was -0.146 and indicated by red pixel. On the other hand, in D-10 with the largest quantity of algal emergence with 2,273,800 cells/mL, the index value was 1.41 and indicated by green pixel (Figure 16). Therefore, it can be considered that the severity of algal bloom emergence is higher at green than red.

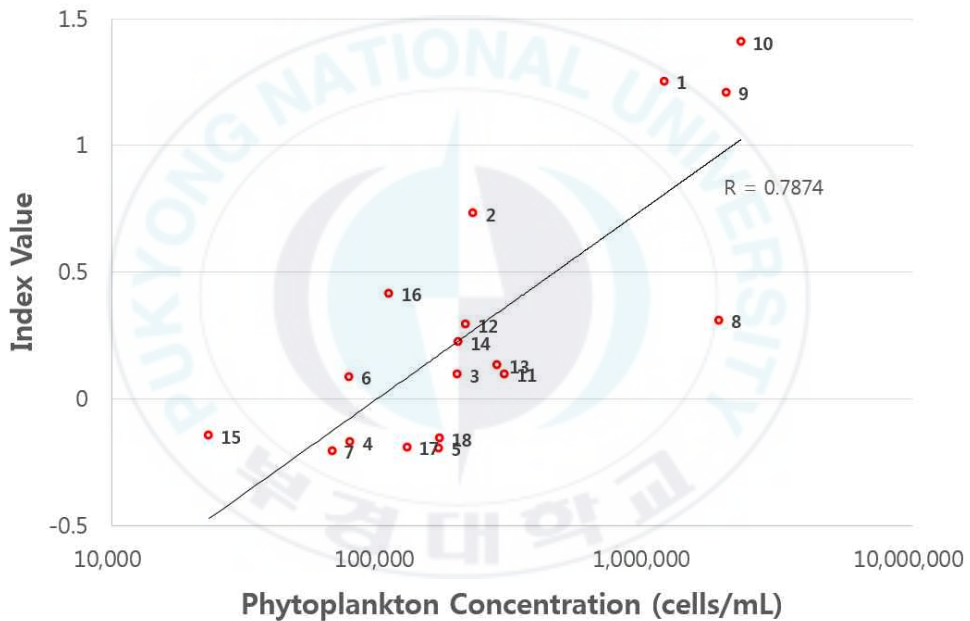


Figure 16. Correlation analysis result between phytoplankton concentration and algal bloom index value.

The residuals in the regression line were found to be relatively higher than the other points in the order D-8, D-2, D-1, and D-16. These results suggest that the aquatic plants were distributed around the sampling point (Figure 17), and that under- or over-detection was detected due to the influence of aquatic plants on the calculation of the algae bloom detection index in the image.



Figure 17. Sampling sites where aquatic plants are distributed :  
(a) D-1, (b) D-2, (c) D-8 and (d) D-16.

### 3.3 The emergence aspects of phytoplankton

In Korea, algae warnings have been implemented since 1988 to secure safety of water supply source. Algae warnings are issued into Watch, Warning and Algal Bloom by classifying the degree of algal bloom emergence (MOE, 2015). For the Algae Warnings Index, concentration of chlorophyll-*a* and quantity of harmful cyanobacteria cells are used. The criteria for issuing algae warnings in 2015, the year this study conducted, are shown in Table 5.

Table 5. Criteria and indicators of algae bloom warning system

	Chlorophyll- <i>a</i> (mg/m <sup>3</sup> )	Cyanobacteria(cells/mL)
Watch	15	500
Warning	25	5,000
Algal Bloom	100	1,000,000

By applying the detection index to the above criteria, the study identified the spatial distribution of algal bloom in the investigated area. Algae warnings have been issued based on determined spatial distributions. In July 29<sup>th</sup> 2015, the detection area of algal bloom was 0.33 km<sup>2</sup>. A Watch level (less than 5,000 cells/mL) was not detected. A Warning level (5,000 - 1,000,000 cells/mL) was detected for an area of 0.30 km<sup>2</sup> (91.41%), and an Algal Bloom level (greater than 1,000,000

cells/mL) was detected for an area of 0.03 km<sup>2</sup> (8.59%). This emergence of algae was the highest at both river banks and at the left side of the water within the image corresponding to the downstream of the river (Figure 18a). On August 18<sup>th</sup> 2015, the detection area of algal bloom was a total area of 0.31 km<sup>2</sup>. An area with an algae concentration equivalent to the Watch level was not detected. The area with a Warning level concentration was 0.30 km<sup>2</sup> (96.58%) and the area with an Algal Bloom level was 0.01 km<sup>2</sup> (3.42%). The image of August 18<sup>th</sup> data also showed high emergence at both banks of the river (Figure 18b). Comparing the July 29<sup>th</sup> and August 18<sup>th</sup> data, the Warning area, was similar, but the area of Algal Bloom was reduced by 0.02 km<sup>2</sup>, indicating that the occurrence of algal bloom had alleviated by August 18<sup>th</sup>.

Table 6. Occurrence range of algal bloom at 29 July 2015 and 18 August 2015

Phytoplankton concentration (cells/mL)	Occurrence range of Algal Bloom (km <sup>2</sup> )	
	2015.07.29.	2015.08.18
~ 5,000	0	0
5,000 ~ 1,000,000	0.30	0.30
1,000,000 ~	0.03	0.01

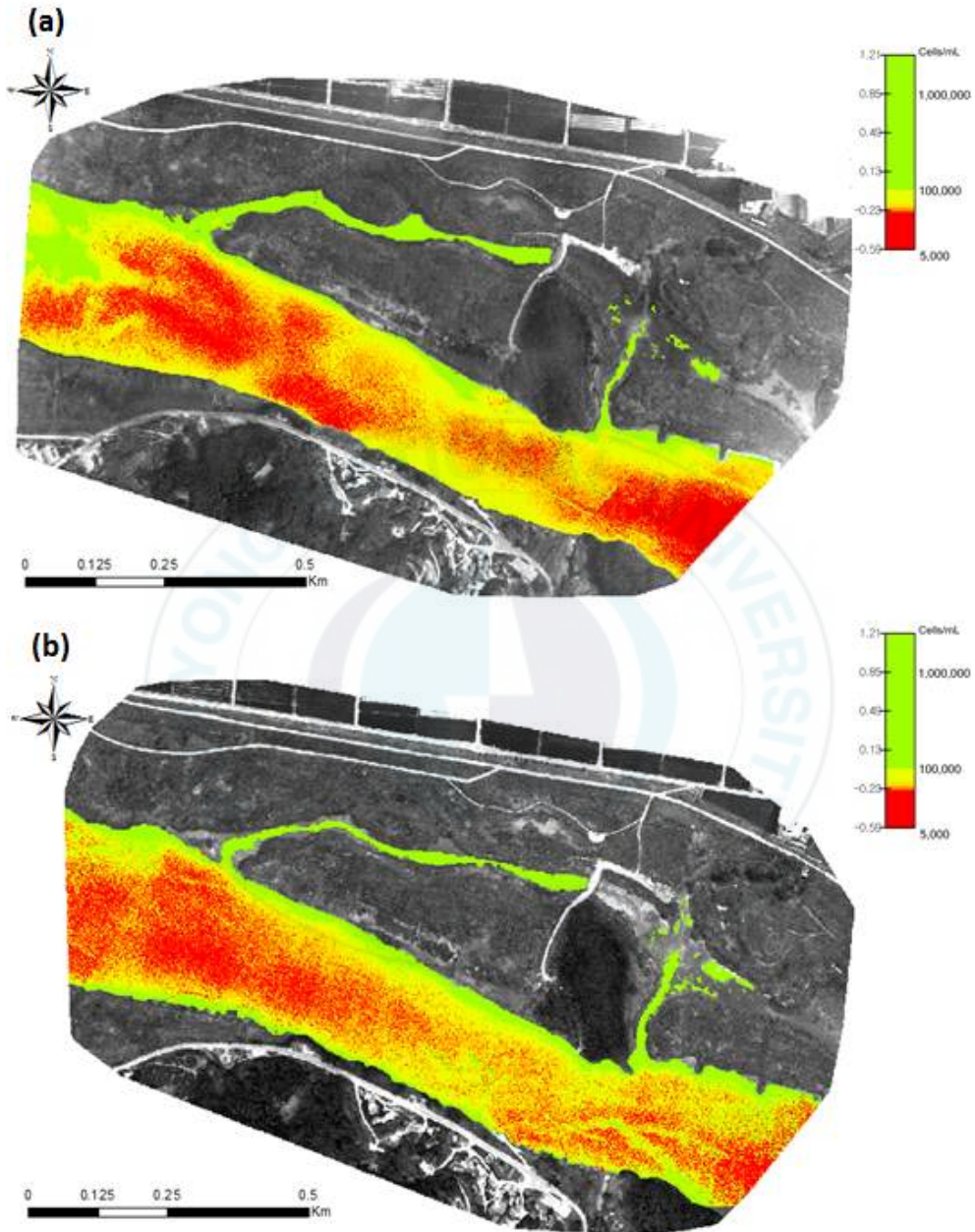


Figure 18. Spatial distribution of algal bloom in the survey area photographed by UAV: (a) 29 July 2015 and (b) 18 August 2015.

## 4. CONCLUSION

Recently, In Korea, the intensity and extent of water pollution becoming serious, caused by algal bloom has currently been bringing serious anxiety of people over safety of water supply sources and it is now being recognized as a national issue. In order to address the anxiety of people over use of drinking water and to supply stable water resources by securing clean water sources, it is urgently needed to develop technologies preventing water pollution caused by algal bloom. Furthermore, it is important to enhance capabilities to deal with emergence and distribution of algal bloom preemptively through regular forecasting and effective monitoring activities.

This study attempted to enhance controlling capability of river water quality and environment by developing algal bloom monitoring technology using UAV which can conduct effective interpretation of spatial distribution at a lower cost. For this purpose, the study obtained remote sensing data using UAV focusing on midstream areas of Nakdong River, with high dependency for water resource use and with frequent emergence of algae related water pollution. Besides, the study conducted spectral reflectance measuring of the sites and analysis of water quality to verify results and to induce algal bloom detection index equation through wavelength band mixing of sensors. The results showed that the algal bloom detection values obtained from wavelength band mixing of red and NIR had highly positive

correlation with algae standing crops at 18 sites. Besides, the result of analyzing spatial distribution of algal bloom on the overall investigated water area showed that the severity in the area from 0.30 km<sup>2</sup> was at the level of Warning (5,000 ~ 1,000,000 cells/mL) in the criteria for issuing algae warnings. This finding may suggest that the algal bloom monitoring technology using UAV presented in this study can be sufficiently utilized for controlling river water quality and environment. However, the study has limitations for verifying the accuracy because it did not consider monitoring of the river before algal bloom emergence and the results are obtained from only two occasions of monitoring. Therefore, in future, to apply the algal bloom remote monitoring technology using UAV in the actual field, it would be necessary to increase the reliability through additional water quality analysis on various water surface conditions depending on the degree of pollution along with continuous research on spectral features.

## 5. REFERENCE

Bates, B. C., Kundzewicz, Z. W., Wu, S., Palutikof, J. P. (Eds.), 2008, Climate change and water, Technical Paper, International panel on climate change (IPCC) Secretariat, Geneva.

Berni, J., Zarco-Tejada, P. J., Suarez, L., Fereres, E., 2009, Thermal and narrowband multispectral remote sensing for vegetation monitoring from an unmanned aerial vehicle, IEEE Transactions on Geoscience and Remote Sensing, Vol. 47, pp. 722-738.

Boyer, G. L., 2006, Monitoring harmful algal blooms in the Great lakes, Great Lakes Research Review, Vol. 7. pp. 1-7.

Choe, E. Y., Lee, J. W., Lee, J. K., 2011, Estimation of Chlorophyll-*a* Concentrations in the Nakdong River Using High-Resolution Satellite Image, Korean Journal of Remote Sensing, Vol, 27, NO. 5, pp. 613-623.

Dekker, A.G., 1993. Detection of optical water quality parameters for eutrophic waters by high resolution remote sensing, Netherlands, Vrije University Amsterdam, Doctor's thesis.

Del Pozo, S., Rodríguez-Gonzálvez, P., Hernández-López, D.,

Felipe-García, B., 2014, Vicarious radiometric calibration of a multispectral camera on board an Unmanned Aerial System, *Remote Sensing*, Vol. 6, pp. 1918-1937.

Dunford, R., Michel, K., Gagnage, M., Piègay, H., Trèmelo, M. L., 2009, Potential and constraints of Unmanned Aerial Vehicle technology for the characterization of Mediterranean riparian forest, *International Journal of Remote Sensing*, Vol. 30, pp. 4915-4935.

E-today News, 2015, This year algal bloom occurred at the Dodong Pier in the Nakdong River, June 10.

Everaerts, J., 2008, The use of Unmanned Aerial Vehicles (UAVs) for remote sensing and mapping. In proceeding of the International Archives of the Photogrammetry, Remote Sensing and Spatial Information Sciences, Beijing, China, 5-7 July, pp. 1187-1192.

Hakala, T., Suomalainen, J., Peltoniemi, J. I., 2010, Acquisition of bidirectional reflectance factor dataset using a micro unmanned aerial vehicle and a consumer camera, *Remote Sensing*, Vol. 2, pp. 819-832.

Han X. and Zheng W., 2010, Chlorophyll-*a* estimation using satellite observations in tai lake, China, *Proceeding of International Conference on Multimedia Technology(ICMT)*, pp. 1-4.

Jang, H. S., Roh, T. H., 2005, Extraction of horizontal alignment information using rc helicopter photogrammetric system, Journal of the Korean Association of Geographic Information Studies, Vol. 8, No. 4, pp. 44-51.

Jang, S. W., Kim, D. H., Seong, K. T., Chung, Y. H., Yoon, H. J., 2014, Analysis of floating debris behavior in the Nakdong River basin of the southern Korean peninsula using satellite location tracking buoys, Marine Pollution Bulletin, Vol. 88, pp. 275-283.

Jang, S. W., Lee, S. K., Kim, D. H., Chung, Y. H., Yoon, H. J., 2015, Application of remote environmental monitoring technique to efficient management of beach litter, International Journal of u- and e-Service, Science and Technology, Vol. 8, No. 7, pp. 357-368.

Jang, S. W., Lee, S. K., Oh, S. Y., Kim, D. H., Yoon, H. J., 2011, The application of unmanned aerial photography for effective monitoring of marine debris, Korean Society of Marine Environment and Safety, Vol. 17, pp. 307-314.

Kim, B. C., Kim, D. S., Kwon, O. K., 1989 The trophic state of Lake Paldang, Korean Society on Water Quality, 5, pp. 39-46.

Kim, H. W., Ha, K., Joo, G. J., 1998, Eutrophication of the lower Nakdong River after the construction of an estuarine dam in 1987, *International Review of Hydrobiology*, Vol. 83, pp. 65-72.

Kim, Y. M., Byun, Y. G., Huh, Y., Yu, K.Y., 2007, Detection of *cochloidium polykrikoides* red tide using MODIS level 2 data in coastal waters, *Journal of the Korean Society of Civil Engineers*, Vol. 27, pp. 535-540.

Kim, Y. S., Suh, A. S., Jo, M. H., 1998, *Introduction to remote sensing*, Dong Hwa technology publishing Co.

Kutser T., Metsamaa L., Strömbeck N., Vahtmäe E., 2006, Monitoring cyanobacterial blooms by satellite remote sensing, *Coastal and Shelf Science*, Vol. 67, pp. 303-312.

Laliberte, A. S., Rango, A., Herrick, J. E., Fredrickson, E. L., Burkett, L., 2007, An object-based image analysis approach for determining fractional cover of senescent and green vegetation with digital plot photography, *Journal of Arid Environments*, Vol. 69, pp. 1-14.

Ministry of Environment, 2015, Systematic algal bloom management through the improvement of algae warnings. Press release (in Korean) (2015)

Ministry of Environment- Water Information System,  
<http://water.nier.go.kr>

Ministry of Environment, 2010, Study on preparation a master plan for reduction of algal of freshwater in Korea.

Ministry of Environment- Nakdong River Basin Environmental Office.  
<http://www.me.go.kr/ndg/>

Mishra S, Mishra D R and Schluchter W M, 2009, A novel algorithm for predicting PC concentrations in cyanobacteria : a proximal hyperspectral remote sensing approach. Remote Sensing, Vol. 1, pp. 758-775.

Mishra S, Mishra D R and Lee Z P and Tucker C G 2013, Quantifying cyanobacteria phycocyanin concentration in turbid productive waters: a quasi-analytical approach. Remote sensing of Environment, Vol. 133, pp. 141-151.

Office of the Secretary of Defense, 2003, Unmanned Aerial Vehicles Roadmap.

Park, S. H., 2015, Quantifying the algal blooms, the obliterated

Nakdong River: A study of the controversy over the four major river project and the alger blooms, Korea, Seoul National University, Master's thesis.

Paerl, H. W., Huisman, J., 2008, Blooms like it hot, Science, Vol. 320, pp. 57-58.

Park, H. G., 2014, The occurrences and reduction measures of algal bloom, Bulletin of Korea Environmental Preservation Association, No. 412, pp. 17-21.

Park, S. B., 2012, Algal blooms hit South Korean rivers. Nature news.

Park, S. J., 2014, A Study on the Possibility of Solid Fuel with Algae in Ash Pond of Thermal Power Plant, River, Lake and Marsh, Korea, Keimyung University, Master's thesis

Reinart A., Kutser T., 2006, Comparison of different satellite sensors in detecting cyanobacterial bloom events in the Baltic Sea, Remote sensing of Environment, Vol. 102, pp. 74-85.

SBS TV, 2012, Nakdong River in Youngnam region, fatigue by extreme toxic algae. August 8.

SBS TV, 2013 Nakdong River 'Late autumn algal bloom' and 'Dead fish'. November 6.

Senhorst, H. A. J., Zwolsman, J. J. G., 2005, Climate change and effects on water quality: A first impression, *Water Science and Technology*, Vol. 51, 5, pp. 53-59.

Sensefly, <https://www.sensefly.com>.

Simis S, Peters S and Gons H, 2005, Remote sensing of the cyanobacterial pigment phycocyanin in turbid inland water, *Limnology and Oceanography*, Vol. 50. pp. 237-245.

Srivastava, A., Ahn, C. Y., Asthana, R. K., Lee, H. G., Oh, H. M., 2015, Status, alert system, and prediction of cyanobacterial bloom in South Korea, *Biomed Research International*, Vol. 2015. pp. 1-8

Su, T. C., Chou, H. T., 2015, Application of multispectral sensors carried on unmanned aerial vehicle (UAV) to trophic state mapping of small reservoirs: A case study of Tain-Pu reservoir in Kinmen, Taiwan, *Remote Sensing*, Vol. 7, pp. 10078-10097.

Thackeray, S. J., Jones, I. D., Maberly, S. C., 2008, Long-term change in the phenology of spring phytoplankton: Species-specific responses

to nutrient enrichment and climatic change, *Journal of Ecology*, Vol. 96, 3, pp. 523–535.

Tianyun, X., Xiaocheng, T., Defang, Y., Yonghe, X., Hongliang, Y., 2015, UAV remote sensing applications in large-scale mapping in the hilly region of Tibetan Plateau, *International Journal of Control and Automation*, Vol. 8, No. 3, pp. 279–286.

Yonhap News, 2014, The first algal bloom occur in middle basin of Nakdong River, May 30.

Yonhap News, 2015, Algal bloom occur everywhere in the Nakdong River including Haman Barrage, June 16.